Supplementary Information

Molten aluminum doping porous silicon anodes enable high initial coulombic efficiency and stability

Xiangshun Yan,[a,b] Yuan Chen,*[a] Yongshu Wang,[a,b] Fan Wu,[a,b] Wensheng Wang,[a,b] Wei Zhang,[a,b] Xin Yang,[b] Zhongchao Bai,[a] Chao Dong,[c] Antonio Moore[d] and Qiang Zhang[a]

[a] College of Mechanical and Electronic Engineering, Shandong University of Science and Technology, Qingdao 266590, China

[b] College of Energy Storage Technology, Shandong University of Science and Technology, Qingdao 266590, China

[c] Department of Chemistry and Physics, The University of Texas of the Permian Basin, 4901 E University Blvd Odessa TX 79762, USA

[d] Department of Life and Physical Sciences, Fisk University, 1000 17th Ave N Nashville TN 37208, USA

Methodology

1. The synthesis of pSi-Al

The pSi-Al samples were synthesized by a low-temperature molten salt reaction. Briefly, 1g Mg2Si and 3g AlCl3 were sealed in autoclave with Ar protective gas. Then, run it in a high-temperature furnace for 5 h at 300 ℃. After that, the samples were removed and washed several times with deionized water and hydrochloric acid. First, the samples were acid washed using excess concentrated hydrochloric acid (36~38 %) for 4 h. Subsequently, It was settled and the supernatant was removed. Washed with excess deionized water for 30 min and repeated several times until the supernatant was clear. Ultimately, it was dried and the pSi-Al was produced. For comparison, the reaction temperatures were experimentally controlled as 250 ℃, 350 ℃, 400 ℃, and 450 ℃, respectively, and other steps remained the same. Moreover, the commercial silicon powder (Si-Nps) was used for comparison (50 nm, BTR New Material Group Co., Ltd).

2. Material characterization

The crystalline properties of samples were investigated using X-ray powder diffraction (D8 Advance X-ray diffractometer, Cu Kα radiation). Field emission scanning electron microscopy (SEM, APREO, America), transmission electron microscopy (TEM, FEI Tecnai F20) for morphology and internal structure, and energy dispersive X-ray spectroscopy (EDX) for elemental analysis were used to analyze the samples. The specific surface area, pore volume were measured using an automated gas adsorption analyzer BET (Hiden IGA100B). X-ray photoelectron spectroscopy (XPS, Thermo Kalpha) was employed to investigate the elemental valence states and chemical components of the sample surface. Inductively coupled plasma mass spectrometry (ICP-MS, PerkinElmer NexION 300X) was used to detect specific levels of elements.

3. Electrochemical measurements

The electrochemical performance of the pSi-Al was examined in the battery channel. It was constructed into a CR2032 type button cell in a glove box filled with Ar (O_2 < 0.01 ppm, H_2O < 0.01 ppm). The anode material was first combined in a 7:1.5:1.5 ratio with conductive carbon black and polyacrylic acid (PAA) to create the anode

slurry. After that, a scraper was used to apply this evenly to the copper foil, and the electrode was dried in a drying oven at 60 ℃ for 24 hours. Using a slicing machine, the working electrodes were punched into discs with a diameter of 12 mm. The mass loading of the electrode was around 0.8~1.2 mg cm^{-2}. Ultimately, CR2032 button half-cells were assembled in the glove box, using a solution of ethylene carbonate (EC) and diethyl carbonate (DEC) containing 1.0 M $LiPF_6$ (v:v=1:1) as the electrolyte, microporous polypropylene membrane (Celgard 2400) as the diaphragm, and lithium metal foil as the counter electrode. After a 12-hour rest period, constant current charge/discharge test was performed on the NEWARE CT-4000-5V channel with a cut-off voltage (vs Li^+/Li) of 0.01~1.5 V.

Cyclic voltammetry (CV) measurements were performed with a CHI660D electrochemical workstation at a scan rate of 0.1 mV s^{-1} over a voltage window of 0.01~1.5 V. Electrochemical impedance spectroscopy (EIS) was conducted between 0.01 and 100 kHz in frequency and at a measuring voltage of 10 mV. Galvanostatic intermittent titration technique (GITT) was used to discharge and charge the half-cells using the NEWARE test channel at a current density of 200 mA g^{-1}, with a current pulse duration of 20 min and an interval of 3 h.

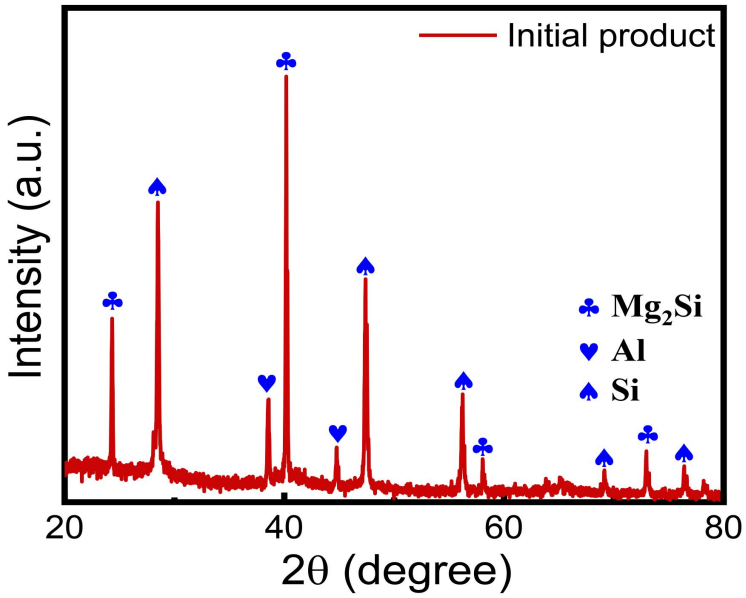

Fig. S1 XRD image of initial product.

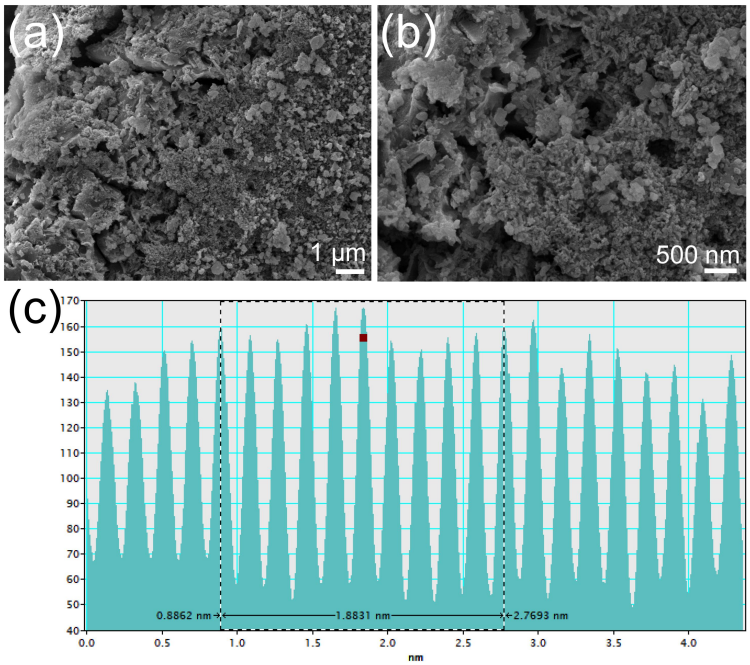

Fig. S2 SEM images of SA300 (a) 1 um. (b) 500 nm. (c) Lattice spacing calculation from HRTEM.

Address correspondence to Yuan Chen, email: chenyuan@sdust.edu.cn.

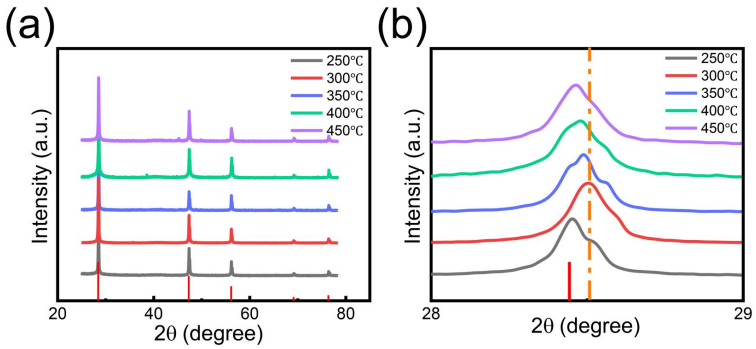

Fig. S3 (a) XRD images at different temperatures. (b) Enlargement images.

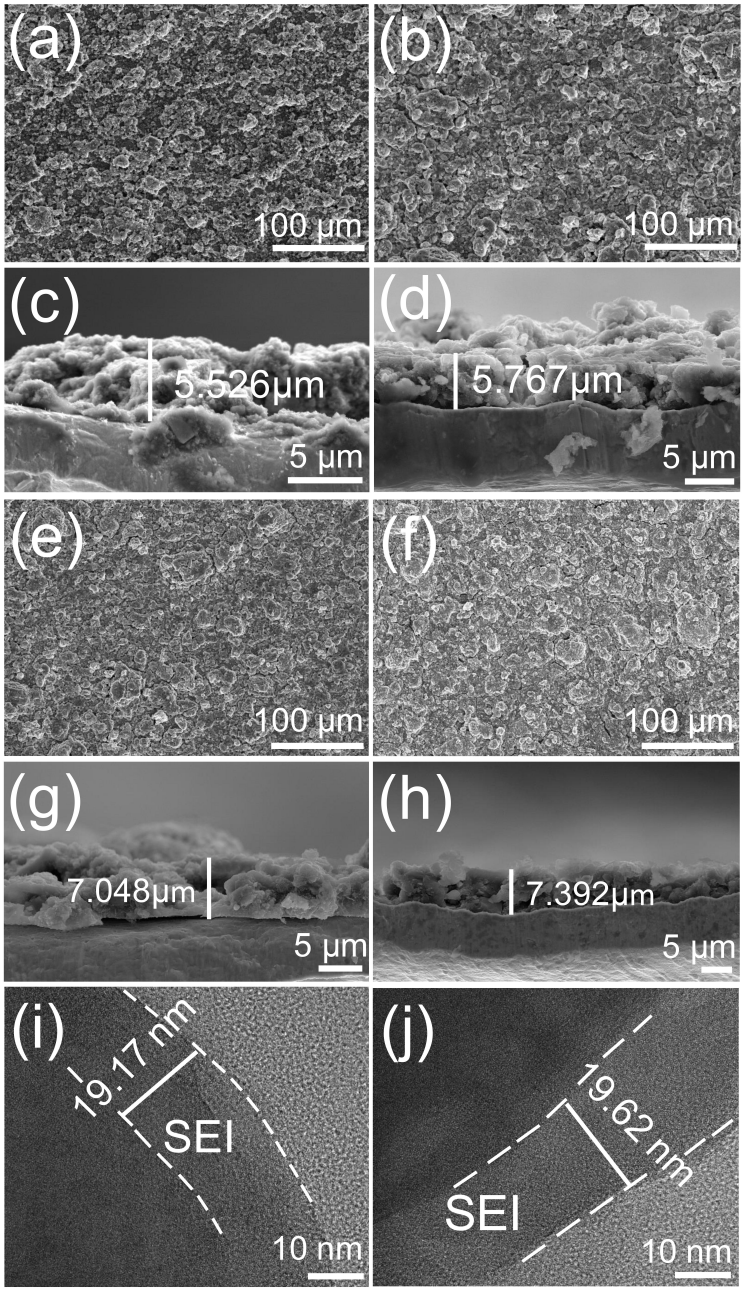

Fig. S4 SEM images of the electrodes. (a) SEM image of SA300 before cycling. (b) SEM image of SA300 after the first cycle. (c) Cross-sectional SEM image of SA300 before cycling. (d) Cross-sectional SEM image of SA300 after the first cycle. (e) SEM image of SA250 before cycling. (f) SEM image of SA250 after the first cycle. (g) Cross-sectional SEM image of SA250 before cycling. (h) Cross-sectional SEM image of SA250 after the first cycle. (i) TEM image of SA300 after the first cycle. (j) TEM image of SA250 after the first cycle.

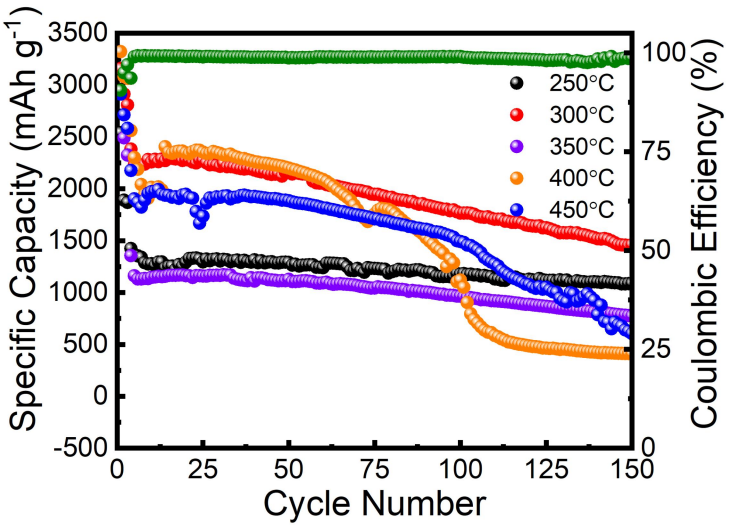

Fig. S5 Cycle performances of SA250, SA300, SA350, SA400 and SA450 at 1.0 A g^{-1}.

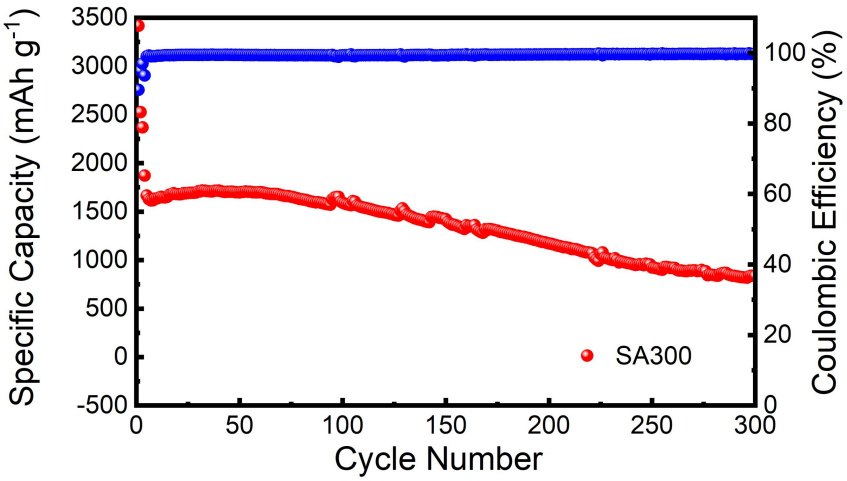

Fig. S6 Cycle performance of SA300 at 1.0 A g^{-1}.

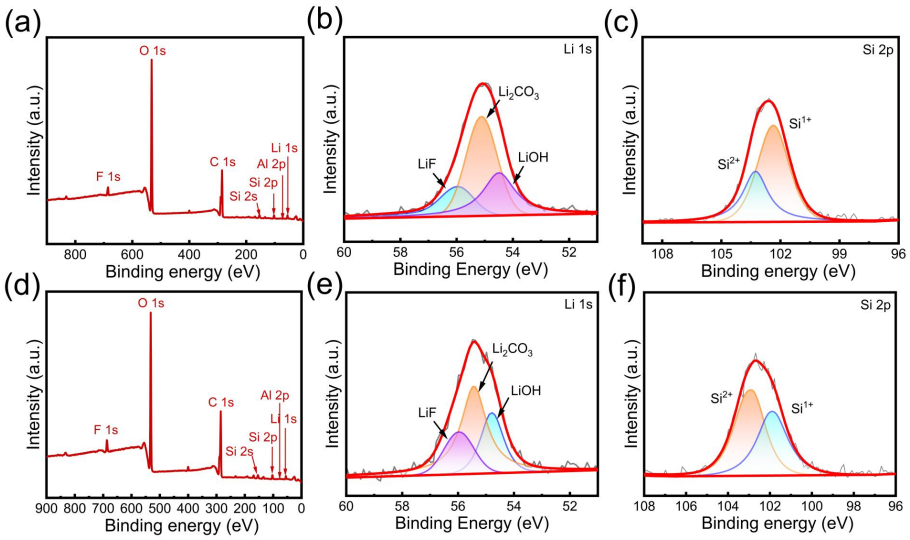

Fig. S7 XPS analysis of electrodes after 100 cycles. (a) XPS survey of SA250. (b) Li 1s high-resolution XPS spectra of SA250. (c) Si 2p high-resolution XPS spectra of SA250. (d) XPS survey of SA300. (e) Li 1s high-resolution XPS spectra of SA300. (f) Si 2p high-resolution XPS spectra of SA300.

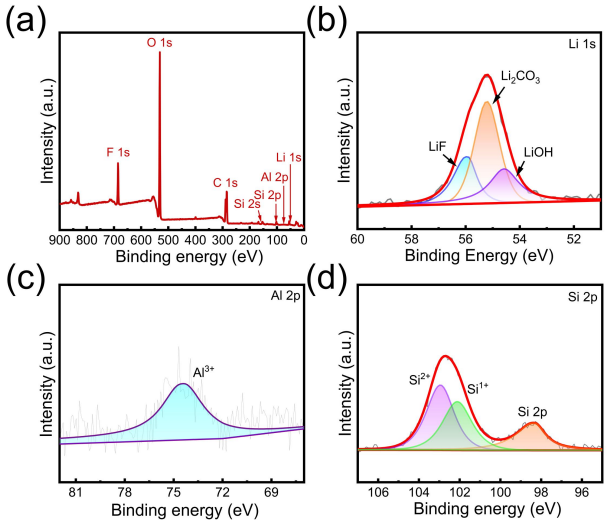

Fig. S8 XPS analysis of SA300 after the first cycle. (a) XPS survey. (b) Li 1s high-resolution XPS spectra. (c) Al 2p high-resolution XPS spectra. (d) Si 2p high-resolution XPS spectra.

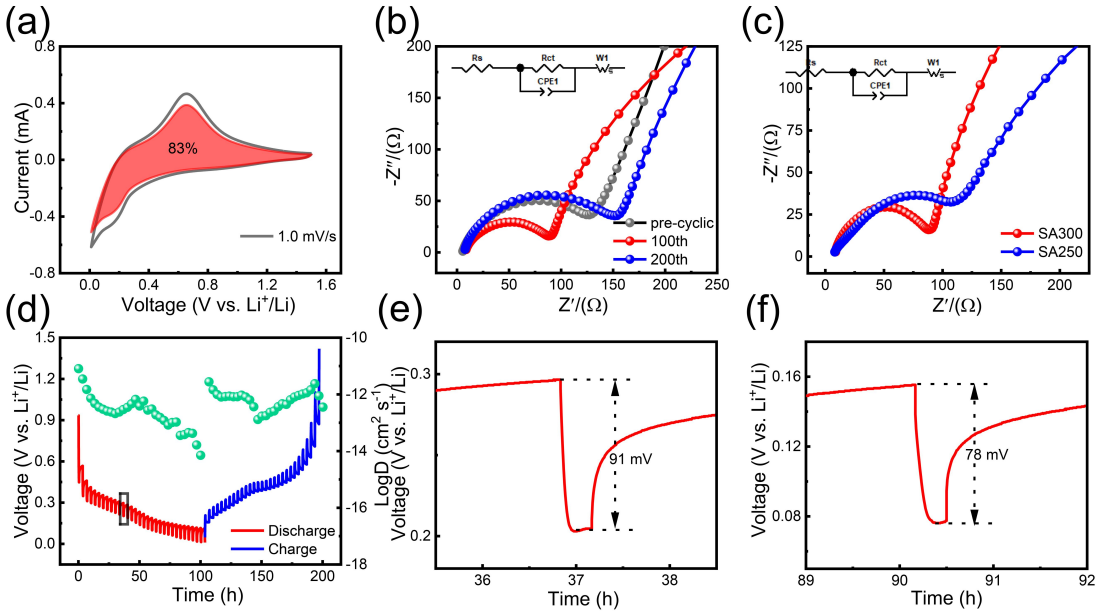

Fig. S9 (a) Capacitance control percentage of SA300 at 1.0 mV s^{-1}. (b) EIS comparison of SA300 before, at the 100th and 200th cycles. (c) EIS comparison of SA300 and SA250 at the 100th cycle. (d) GITT curves and calculated D values from GITT of SA250. (e) Enlargement image of SA250. (f) Enlargement image of SA300.

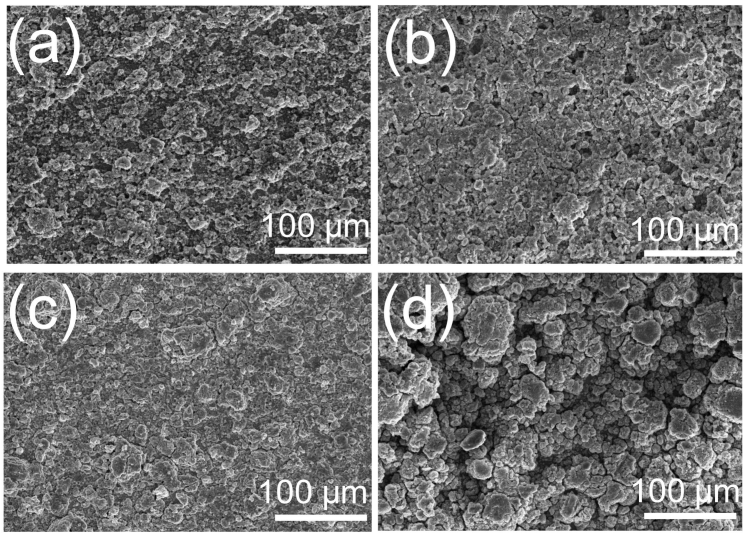

Fig. S10 SEM images of electrode. (a) SA300 before cycling. (b) SA300 after 100 cycles. (c) SA250 before cycling. (d) SA250 after 100 cycles.